PHYSICAL REVIEW C VOLUME 18, NUMBER 1 JULY 1978

Multiplicity of the γ cascades in the ^{61}Cu continuum: Dependence on excitation energy of the entry states*

J. H. Barker†
Department of Physics, Saint Louis, University, St. Louis, Missouri 63103

D. G. Sarantites
Department of Chemistry, Washington University, St. Louis, Missouri 63130

Ö. Skeppstedt, E. Wallander, G. Alenius, and S.-E. Arnell
Department of Physics, Chalmers University of Technology, Gothenburg, Sweden

(Received 9 June 1977)

The multiplicity of the γ cascades in the ^{61}Cu continuum entering 17 levels populated via the ^{58}Ni(^{4}He,$p\gamma$)^{61}Cu reaction have been measured for incident ^{4}He energies of 17.0 and 19.5 MeV. A general trend of increasing multiplicity of side feeding with increasing excitation energy of the entry states is established. For excitations between 6.0 and 12.5 MeV in ^{61}Cu the side-feeding multiplicities vary between 1.2 and 4.0, while the total multiplicities vary between 4.0 and 6.8. The side-feeding multiplicities from the 19.5-MeV experiment are about 0.7 units higher than those from the 17.0-MeV experiment. Detailed statistical model calculations which include explicitly γ-ray competition reproduce the trends and the magnitudes of the measured multiplicities.

[NUCLEAR REACTIONS ^{58}Ni(α,$p\gamma$), 17.0 and 19.5 MeV; measured γ-ray multiplicities vs E^*; compound statistical model analysis.]

I. INTRODUCTION

The reaction ^{58}Ni(^{4}He, $p\gamma$) ^{61}Cu has been used extensively to study both the structure[1,2] of ^{61}Cu and the details of the compound statistical model including γ-ray decay.[3,4] As a consequence of that work, a highly detailed decay scheme including level energies, spin and parity assignments, branching ratios, and nuclear-level lifetimes exists for ^{61}Cu. In addition, compound-statistical model parameters have been deduced based on detailed measurements of cross sections for many individual levels following the (^{4}He, $p\gamma$) reaction.

In a more recent study[5] Sarantites and Barker have reported the lifetimes for γ decay of the continuum states to discrete states in ^{61}Cu. From a measurement of the reduction of the observed Doppler shift of γ rays deexciting levels of known lifetime, it was concluded[5] that the multiplicity of γ rays in the continuum decay increased with increasing excitation energy of the entry states in the γ cascade. The conclusion was based on the observed increase in the continuum feeding times as a function of increasing excitation energy of the entry states in the cascades in the ^{61}Cu nucleus.

Recently several groups[6-8] have reported on the direct measurement of γ-ray multiplicities via a multi detector γ-γ coincidence technique. Most of that work has employed heavy-ion induced reactions in the deformed region of nuclei. In the present work we have extended this type of experiment to light nuclei and have included a coincidence requirement with charged particles to establish a dependence with excitation energy. In an earlier work Degnan *et al.*[9] have reported average multiplicities for ^{61}Cu and other nuclei as a function of E^*. Since that work[9] did not employ coincidences with a Ge(Li) detector their results did not select the level or in some cases the product nucleus observed.

In this work a Ge(Li) detector and two Si proton detectors were employed in coincidence in order to establish the excitation energy in ^{61}Cu following the ^{58}Ni(^{4}He, $p\gamma$) reaction. Two or seven NaI detectors were added and multiple coincidences between the Ge(Li)-Si pairs and any number of NaI detectors were recorded. From the latter coincidence information the multiplicity of the cascades that start from a given excitation and lead to 17 states in ^{61}Cu were deduced. The results are compared with detailed theoretical calculations based on the predictions of the compound-statistical model for nuclear reactions.

II. EXPERIMENTAL METHODS

Two independent measurements are reported in this paper. The first is an experiment utilizing a beam of 20.0-MeV ^{4}He^{++} from the Washington University cyclotron and the second is a 17.5-MeV ^{4}He^{++} experiment performed at the Uppsala tandem accelerator.

TABLE I. Multiple coincidence probabilities $P_{ip}^{(\alpha)}$ for the ^{58}Ni(^{4}He,$p\gamma$)^{61}Cu reaction at 19.5 MeV. The underlined numbers are statistical errors and refer to the least significant figures indicated.

Level energy (keV)	γ-ray energy (keV)	fold p	$P_{ip}^{(\alpha)} \times (100)$ E^* ^{61}Cu (MeV) 12.5		10.5		8.5		6.4	
475.0	475	0	89	15	79	10	86	7	86	7
		1	9	5	20	6	13	3	13	3
		(2–7)	3	2	1	1	1	1	1	1
1394.1	1394.1	0	73	5	77	4	77	6	86	10
		1	24	3	22	2	21	3	14	4
		(2–7)	3	1	1	1	2	1	0	1
1942.4	632.0	0	73	9	75	8	82	10	65	16
		1	22	5	23	3	18	5	33	9
		(2–7)	5	2	2	1	0	1	1	2
2295.0	900.0	0	70	10	74	10	76	11	88	20
		1	26	5	23	4	22	5	11	9
		(2–7)	4	1	3	1	2	2	1	2
	562.5	0	74	14	79	8	78	9	84	17
		1	21	6	20	5	21	4	14	8
		(2–7)	5	2	1	1	1	1	1	3
	352.7	0	61	9	74	9	77	11	79	13
		1	33	5	23	4	21	8	18	7
		(2–7)	7	2	3	1	2	1	2	2
2336.2	1025.8	0	78	7	75	5	78	6	84	18
		1	21	4	22	3	19	3	16	6
		(2–7)	1	1	2	1	3	1	1	2
	1366.2	0	76	7	75	4	81	5	82	8
		1	23	3	23	2	18	3	18	4
		(2–7)	2	1	2	1	1	1	0	1
2583.6	851.1	0	63	13	67	7	67	13	75	19
		1	33	6	30	4	30	7	25	10
		(2–7)	4	2	3	1	2	1	0	2
2611.8	669.5	0	75	12	73	8	73	8	77	15
		1	21	7	26	4	26	4	22	6
		(2–7)	3	1	1	1	2	1	1	2
	879.3	0	71	7	75	4	75	5	81	10
		1	26	3	22	2	24	3	19	6
		(2–7)	3	1	3	1	1	1	0	1

TABLE I. (*Continued*)

Level energy (keV)	γ-ray energy (keV)	fold p	$P_{lp}^{(\alpha)} \times (100)$ E^* ^{61}Cu (MeV) 12.5		10.5		8.5		6.4	
2626.8	1316.4	0	77	12	78	8	79	7	76	9
		1	22	3	21	3	19	3	23	4
		(2–7)	2	1	1	1	1	1	1	1
2923.9	1191.4	0	79	30	76	13	83	13	77	19
		1	16	13	24	8	17	7	23	9
		(2–7)	6	3	0	1	0	1	0	1
3015.6	1705.2	0	77	8	81	6	81	10	91	23
		1	21	4	17	3	18	4	9	9
		(2–7)	2	1	2	1	1	1	0	1
3259.6	647.8	0	79	10	68	6	65	8	72	15
		1	19	5	28	3	34	5	27	8
		(2–7)	2	1	4	1	1	1	1	2
	1527.1	0	66	7	77	9	98	14	89	24
		1	29	5	20	5	2	6	11	11
		(2–7)	5	1	3	1	0	1	0	2
3739.4	1444.4	0	78	10	73	7	87	12	69	23
		1	20	4	25	3	13	4	31	12
		(2–7)	2	1	1	1	0	1	0	1
3942.4	1222.2	0	76	10	77	7	86	10	88	13
		1	21	4	21	3	14	4	12	7
		(2–7)	3	1	1	1	0	1	0	1
4081.8	1361.6	0	71	7	73	5	73	7	68	10
		1	27	4	25	3	23	4	29	6
		(2–7)	2	1	1	1	4	1	3	1

A. 19.5-MeV experiment

The basic scattering chamber and associated electronics will be described in detail in a forthcoming paper[10]; only the essential features will be presented here. The multicoincidence arrangement involved a Ge(Li), two charged particle detectors, and seven NaI detectors. A Ge(Li) detector (7% efficient for 1332 keV relative to a 7.6-cm×7.6-cm NaI detector at 25 cm) was located 8.5 cm from the target at 90° to be beam. Here we use a spherical polar coordinate system[11] with its origin at the target, its axis ($\theta = 0°$) coinciding with the beam, and the azimuthal angle ϕ taken to be 0° for the horizontal plane containing the Ge(Li) detector. Two charged particle detectors (300 mm^2 area by 1000 μm thick) were located 4 cm above and below the target ($\theta_1 = \theta_2 = 90°$, $\phi_1 = 90°$, and $\phi_2 = 270°$). The seven 5.1-cm diam. by 7.6-cm long NaI detectors were placed at a distance of 10 cm from the target, each with its symmetry axis passing through the target. Four of these were located in the reaction plane at (θ, ϕ) of (50°, 0°), (140°, 0°), (225°, 0°), and (315°, 0°). Two of the remaining three were above the reaction plane at (θ, ϕ) of (69°, 139°) and (111°, 139°), and the last one below the plane at (θ, ϕ) of (69°, 221°). The Ge(Li) and NaI detectors were inserted in two

specially cast Pb shields that insured a minimum of 2 cm of Pb between adjacent detectors. This was sufficient to reduce crystal-to-crystal scattering to a negligible amount.

The target was a uniform 5.0-mg/cm^2 self-supporting Ni foil enriched to 99.95% in ^{58}Ni. This thickness gave a target-center energy of 19.5 MeV for the incident beam of 20.0-MeV ^{4}He^{++}.

An external logic module[10] constructed upon the overlap coincidence technique processed the discriminator signals derived from the Ge(Li) and NaI detectors. It provided digital address information corresponding to the order of observed coincidence for zero, one, two, and three or more fold, depending whether zero, one, two, and three or more NaI detectors fired in coincidence with a Ge(Li)-Si coincidence pair. This information along with the linear signals from the Ge(Li) and the charged particle detectors were stored in the event-by-event mode as 24 bit words on the magnetic tape with the aid of a Nuclear Date 50/50 analyzer interfaced to a PDP-8/L computer. Calibrations of the system are described in detail in Ref. 8. Ge(Li) γ-ray spectra selected according to order of multiplicity and proton-energy window were created off line. These spectra were then analyzed for individual peak areas from the various coincidence folds. The results of this procedure are summarized in Table I as the probabilities $P_{7p}^{(\alpha)}$ for each transition defined by

$$P_{7p}^{(\alpha)} = \frac{C_p^{(\alpha)}}{\sum_{p=0}^{(7)} C_p^{(\alpha)}} , \tag{1}$$

where $C_p^{(\alpha)}$ is the peak area obtained for the αth γ ray in the spectrum corresponding to a p-fold coincidence. The results are presented as four proton-energy groups 2 MeV wide centered on excitation energies of 12.5, 10.5, 8.5, and 6.4 MeV in ^{61}Cu.

B. 17.0-MeV experiment

This experiment involved a four parameter arrangement. It consisted of a 10% Ge(Li) located 7.3 cm from the target directly along the beam axis; a single annular charged-particle detector (200 mm^2 area by 1000 μm thick) located coaxially with the beam and 0.9 cm upstream from the target and two 12.7-cm diam by 15.2-cm long NaI detectors located at 14 cm at angles of ±55° in the reaction plane. Again lead shielding was utilized to reduce crystal to crystal scattering to a negligible amount. The beam was stopped in 0.5-mm Ta absorber in front of the Ge(Li) detector.

The target was a uniform 5.0-mg/cm^2 self-supporting Ni foil enriched to 99.95% in ^{58}Ni. The center-target energy in this experiment was of 17.0 MeV for an incident energy of 17.5 MeV ^{4}He^{++}.

The data from this experiment were acquired as four parameter spectra with the aid of an on-line computer and were stored in the event-by-event mode on magnetic tape. Spectra corresponding to selected coincidence folds and energy windows for the protons were generated off line. The resulting spectra were then analyzed for the desired peak areas. The results of this procedure are presented in Table II for three proton-energy groups 1.65-MeV wide centered on excitation energies of 9.95, 8.3, and 6.67 MeV. The seventh column gives the results for spectra obtained with a gate on the entire proton spectrum from 4.6 to 11.9 MeV of excitation.

III. ANALYSIS AND RESULTS

The probabilities $P_{Np}^{(\alpha)}$ reported in Sec. II are related to the multiplicity of the γ cascade. The probability for a coincidence between the Ge(Li)-Si event pair and one or more of the NaI detectors is related to the number of γ rays available in the cascade. The detailed relationship between $P_{Np}^{(\alpha)}$ and the multiplicity M have been discussed elsewhere.[8,10] Utilizing the notation of Ref. 10 the probability for p our of N detectors firing in coincidence with a gating event α (deexciting the ith bound state and populating the jth state below and coincident with a proton of a given energy) is $P_{Np}^{(\alpha)}$. Following the R method of Refs. 8 or 10, one adds the experimental $P_{Np}^{(\alpha)}$ values to obtain

$$R_p^{(\alpha)} \equiv P_{pp}^{(\alpha)} = \binom{N}{p}^{-1} \sum_{k=p}^{N} \binom{k}{p} P_{Nk}^{(\alpha)} . \tag{2}$$

The quantity $R_p^{(\alpha)}$, so defined, represents the probability for observing a p-fold coincidence if only p NaI detectors were present.

One can readily show that

$$R_p^{(\alpha)} = \sum_{k=0}^{p} (-1)^k \binom{p}{k} (1 - k\bar{\Omega})^{M_{\min}} K_k^{(j)} K_k^{(\text{neut})} , \tag{3}$$

where

$$K^{(0)} = 1 ,$$

$$K_k^{(1)} = (1 - k\Omega_{10}), \ldots, K_k^{(j)}$$

$$= \sum_{q=0}^{j-1} b_{jq} (1 - k\Omega_{jq}) K_k^{(q)} , \tag{3a}$$

and

$$K_k^{(\text{neut})} = (1 - k\Omega_{\text{neut}})^x . \tag{3b}$$

The term $K_k^{(j)}$ of Eq. (3a) represents the contribution to the coincidence probability from known cascades below the gating transition. In the recurrence relation (3a) the ground state is labeled

TABLE II. Multiple coincidence probabilities $P_{2p}^{(\alpha)}$ for the ^{58}Ni(^{4}He,$p\gamma$)^{61}Cu reaction at 17.0 MeV. The underlined numbers are statistical errors and refer to the least significant figures indicated.

Level energy (keV)	γ-ray energy (keV)	fold p	$P_{2p}^{(\alpha)} \times (100)$ E^* ^{61}Cu (MeV) 9.95		8.30		6.67		(4.6–11.9)	
475	475.0	0	91	6	90	4	91	4	91	3
		1–2	9	3	10	3	8	3	9	2
1394.1	1394.1	0	89	5	89	4	91	4	89	3
		1–2	12	3	11	2	9	3	11	2
1732.5	1732.5	0	87	4	88	3	88	4	88	2
		1–2	13	3	12	2	12	2	12	1
	762.4	0	84	8	83	7	84	7	83	5
		1–2	16	5	18	4	16	5	17	3
	421.8	0	85	5	84	4	84	4	84	3
		1–2	16	3	16	2	16	3	16	1
2295.0	984.6	0	91	6	87	4	87	5	88	4
		1–2	10	3	13	2	12	3	12	2
	562.5	0	84	9	84	6	86	9	85	5
		1–2	16	5	16	3	15	5	15	2
2336.2	1366.2	0	87	7	86	6	87	6	86	5
		1–2	14	4	14	3	13	3	13	3
2611.8	879.3	0	86	6	85	4	86	6	85	4
		1–2	14	3	15	2	14	3	15	2
	669.5	0	83	8	83	5	85	8	84	4
		1–2	18	4	18	3	13	3	17	2
2626.8	1316.4	0	84	6	86	5	86	6	86	4
		1–2	15	3	13	2	12	3	13	2
2720.2	1409.9	0	85	5	86	4	87	5	86	4
		1–2	15	3	14	2	13	3	14	2
	987.6	0	84	6	84	4	87	6	85	4
		1–2	17	4	15	3	13	4	15	2
3015.6	1705.2	0	86	7	87	6	88	7	87	5
		1–2	15	4	12	3	12	4	13	2
3259.6	1527.1	0	82	10	86	6	84	8	85	5
		1–2	18	6	15	4	15	5	15	3
	647.8	0	79	9	78	5	80	8	80	5
		1–2	21	5	22	3	18	5	20	2
4081.8	1361.6	0	84	8	86	6	83	8	85	5
		1–2	15	5	15	4	17	5	16	3

TABLE III. γ-ray multiplicities $\langle M_{in}^{(i)}(E^*)\rangle$ for the incoming cascades, and/or $\langle M_{SF}^{(i)}(E^*)\rangle$ for the side feeding as a function of E^* following population via the ^{58}Ni(^{4}He,$p\gamma$)^{61}Cu reaction at 19.5 MeV.

Level energy (keV)	J^π	Side-feeding fraction F_{SF}	M_{out}	γ-ray energy (keV)	$\langle M_{in}^{(i)}(E^*)\rangle$ or $\langle M_{SF}^{(i)}(E^*)\rangle$ E^* (MeV) 12.5	10.5	8.5	6.4	13.5–5.4
4081.8	$(\frac{11}{2}^+)$	1.0	3.3	1361.6	3.9 9	3.1 6	3.3 7	3.4 10	3.4 7
3942.4	$(\frac{11}{2}^-,\frac{9}{2}^+)$	1.0	3.3	1222.2	3.4 12	2.6 10	0.9 30	···	2.4 12
3739.4	$\frac{11}{2}^-$	1.0	3.2	1444.2	2.8 15	3.0 9	···	2.8 21	2.9 12
3259.6	$\frac{11}{2}^-$	1.0	3.0	647.8	2.8 16	4.2 6	3.6 10	2.5 15	3.7 6
				1527.1	5.9 10	3.8 12	···	0.9 40	5.0 4
				Avg.	5.0 11	4.1 5	3.6 10	2.3 14	3.9 5
3015.6	$\frac{11}{2}^-$	1.0	2.4	1705.2	4.1 11	3.2 7	2.6 10	0.7 50	3.2 9
2923.9	$\frac{9}{2}^-$	1.0	2.6	1191.4	4.4 33	3.4 18	2.2 18	2.7 16	3.1 21
2626.8	$\frac{11}{2}^-$	1.0	2.1	1316.4	4.3 8	3.5 6	3.0 6	3.2 8	3.6 7
2611.8	$\frac{9}{2}^-$	0.69	2.5	669.5	3.9 18	3.6 9	3.3 10	2.3 14	3.5 9
				879.3	5.1 8	4.2 6	3.5 7	2.2 12	4.1 7
				Avg.	4.9 7	4.0 5	3.4 6	2.2 9	3.9 6
					(4.4 11)	(3.5 8)	(2.9 9)	(1.8 14)	(3.5 9)
2583.6	$(\frac{9}{2}^-)$	1.0	2.5	851.1	6.4 14	5.3 9	4.9 13	3.0 18	5.4 12
2336.2	$\frac{9}{2}^-$	0.90	2.0	1025.8	4.0 10	4.3 7	3.5 7	2.1 15	3.8 6
				1366.2	4.5 9	4.2 5	2.8 6	2.2 8	3.7 7
				Avg.	4.3 7	4.2 4	3.1 5	2.2 7	3.8 5
					(4.2 8)	(4.2 5)	(3.0 5)	(2.2 9)	(3.7 6)
2295.0	$\frac{9}{2}^-$	0.50	2.2	352.7	6.1 11	3.7 10	2.8 18	2.2 15	3.4 7
				562.5	5.1 16	3.3 13	3.2 10	2.0 21	3.6 11
				900.9	5.4 13	4.4 10	4.3 13	1.8 26	4.5 9
				Avg.	5.8 7	3.8 8	3.5 7	2.1 11	3.9 8
					(7.1 17)	(3.4 16)	(3.4 10)	(0.7 27)	(3.6 18)
1942.4	$\frac{7}{2}^-$	0.49	2.0	632.0	5.5 13	4.3 8	2.6 11	4.9 17	4.3 11
									(3.4 23)
1394.1	$\frac{5}{2}^-$	0.47	1.1	1394.1	5.9 6	4.8 5	4.6 6	2.6 9	4.9 6
					(4.9 16)	(4.8 14)	(4.7 14)	(2.1 23)	(4.9 15)
475.0	$\frac{1}{2}^-$	0.51	1.0	475.0	4.0 16	4.7 14	3.4 7	2.8 7	3.7 11
									(1.6 22)

0. The transitions $j \to q$ have known integral NaI efficiencies Ω_{jq}. The branching ratios b_{jq} for the transitions $j \to q$ satisfy $\sum_{q=0}^{j-1} b_{jq} = 1$.

The $K_k^{(\text{neut})}$ term of Eq. (3b) represents the contribution to the coincidence rate due to response of the NaI detectors (efficiency Ω_{neut}) to x neutrons emitted. Of course, for the (^{4}He,p) reaction studied here, the neutron multiplicity x is zero and thus $K_k^{(\text{neut})} = 1$.

Expanding now Eq. (3) in powers of $\bar{\Omega}$ gives

$$\sum_{r=1}^{M_{in}} \lambda_{pr}^{(j)} X_r^{(i)} = R_p^{(\alpha)} - (1+\lambda_{p0}^{(j)}), \tag{4}$$

where

$$\lambda_{pr}^{(j)} = \frac{1}{r!}\sum_{k=1}^{p} (-1)^{k+r}\binom{p}{k} k^r K_k^{(j)}, \tag{4a}$$

with

$$X_r^{(i)} = \langle M_{in}(M_{in}-1)\ldots(M_{in}-r+1)\rangle \bar{\Omega}^r. \tag{4b}$$

TABLE IV. γ-ray multiplicities $\langle M_{in}^{(i)}(E^*)\rangle$ for the incoming cascades and/or $\langle M_{SF}^{(i)}(E^*)\rangle$ for the side feeding as a function of excitation energy E^* following population via the ^{58}Ni(^{4}He,$p\gamma$)^{61}Cu reaction at 17.0 MeV.

Level energy (keV)	J^π	Side-feeding fraction F_{SF}	M_{out}	γ-ray energy (keV)	$M_{in}(M_{SF})$ E^* (MeV) 9.95	8.3	6.67	11.9–4.6
4081.8	$(\frac{11}{2}^+)$	1.0	3.3	1361.6	...	...	...	1.5 3
3259.6	$\frac{11}{2}^-$	1.0	3.0	647.8	2.9 7	2.5 5	2.0 7	2.3 4
				1527.1	3.2 8	2.4 6	2.3 7	2.6 4
				Avg.	3.1 5	2.4 4	2.1 5	2.5 3
3015.6	$\frac{11}{2}^-$	1.0	2.4	1705.2	2.8 6	2.1 4	2.0 5	2.2 3
2720.2	$\frac{9}{2}^+$	0.64	1.8	987.6	3.2 6	2.6 5	1.8 5	2.4 3
				1409.9	2.9 4	2.5 3	2.3 4	2.6 3
				Avg.	2.9 3	2.5 2	2.1 3	2.5 2
					(3.0 14)	(2.3 12)	(1.7 13)	(2.6 9)
2626.8	$\frac{11}{2}^-$	1.0	2.1	1316.4	2.8 5	2.3 3	2.0 4	2.3 3
2611.8	$\frac{9}{2}^-$	0.73	2.5	669.5	2.6 6	2.5 4	1.3 5	2.1 3
				879.3	2.3 4	2.5 3	2.2 4	2.4 3
				Avg.	2.4 3	2.5 3	1.9 4	2.2 2
					(1.8 12)	(2.1 10)	(1.3 11)	(1.7 7)
2336.2	$\frac{9}{2}^-$	0.94	2.0	1366.2	2.7 5	2.5 3	2.1 4	2.3 3
					(2.6 11)	(2.4 9)	(2.1 9)	(2.2 5)
2295.0	$\frac{9}{2}^-$	0.54	2.2	562.5	2.9 7	2.6 5	2.3 7	2.6 4
				984.6	1.6 4	2.2 3	2.0 4	1.9 3
				Avg.	1.9 4	2.3 3	2.1 4	2.1 3
1732.5	$\frac{7}{2}^-$	0.41	1.4	421.8	3.1 4	3.0 3	3.1 3	3.1 2
				762.4	3.1 7	3.5 5	3.2 5	3.3 4
				1732.5	3.6 3	3.1 2	3.0 3	3.2 2
				Avg.	3.3 2	3.1 2	3.1 2	3.1 2
1394.1	$\frac{5}{2}^-$	0.91	1.1	1394.1	3.1 3	2.9 3	2.4 3	2.8 2
								(2.6 5)
475.0	$\frac{1}{2}^-$	0.78	1.0	475.0	2.5 4	2.6 3	2.2 3	2.5 2
								(2.5 9)

Setting the limit in the sum of Eq. (4) equal to a sufficiently large value p_{max} permits one to solve the system of Eqs. (4) for $X_r^{(i)}$ with $r = 1, 2, \ldots, p_{max}$, and thus obtain $\langle M_{in}\rangle$ from Eq. (4b). The higher amounts of the M_{in} distribution can also be computed.[8,10]

The values for $\bar{\Omega}$ in Eqs. (4) are given by

$$\bar{\Omega} = \Omega_\gamma (1+\alpha_T)^{-1}(1-\Omega_0)^{-1}, \quad (5)$$

where Ω_γ is the integral detection efficiency (full energy and Compton distribution) of one NaI detector for a γ-ray energy E_γ, α_T is the total conversion, and Ω_0 is the integral efficiency of the Ge(Li). The last factor in Eq. (5) corrects the multiplicity[7] for coincidence summing effects in the Ge(Li). For the incoming cascade, the average γ-ray energy $\langle E_\gamma^{(i)}\rangle$ which corresponds to $\bar{\Omega}$ and $\langle M_{in}^{(i)}(E^*)\rangle$ are obtained by requiring that they satisfy simultaneously

$$X_1^{(i)} = \langle M_{in}^{(i)}(E^*)\rangle \bar{\Omega} \quad (6)$$

and

$$\langle E_\gamma^{(i)}\rangle = (E^* - E_{level}^{(i)})/\langle M_{in}^{(i)}(E^*)\rangle, \quad (7)$$

where $E^{(i)}_{\text{level}}$ is the energy of the level which is deexcited by the gating transition.

In the preceding discussion it has been assumed that there are no corrections for angular correlation effects. Estimates of the magnitude of this correction have been made in the same manner as Ref. 8. For the geometries chosen in these experiments the correction factors are essentially unity and therefore this correction was not made.

Tables III and IV summarize the results of the 19.5- and 17.0-MeV experiments, respectively. It must be noted that in all cases $\langle M^{(i)}_{\text{in}}(E^*)\rangle$, the multiplicity of the incoming cascade, has been measured. The first two columns in Tables III and IV give the level energy in keV and its J^π value. The third column gives the fraction of side feeding to each level defined as $F^{(i)}_{\text{SF}} \equiv 1 - \sum_{\text{in}} I_\gamma / \sum_{\text{out}} I_\gamma$. The fourth column gives multiplicity M_{out} of the γ cascade out of the level in question. The fifth column gives the energy of the gating γ ray. Columns six through nine give the deduced multiplicity $\langle M^{(i)}_{\text{in}}(E^*)\rangle$ for the four excitation energies indicated. Second entries given in parentheses refer to the multiplicity $\langle M^{(i)}_{\text{SF}}(E^*)\rangle$ of the side-feeding cascade. The side-feeding cascade refers to the γ cascade which terminates in the level of interest without passing through a known higher lying discrete level. It is the cascade normally calculated via the compound statistical model and differs from the incoming cascade which includes all incoming γ rays without regard to their path. Clearly, if $F^{(i)}_{\text{SF}} = 1$ then $\langle M^{(i)}_{\text{SF}}(E^*)\rangle = \langle M^{(i)}_{\text{in}}(E^*)\rangle$.

If $F^{(i)}_{\text{SF}} < 1$ then $\langle M^{(i)}_{\text{SF}}(E^*)\rangle$ can be deduced from $\langle M^{(i)}_{\text{in}}(E^*)\rangle$ and accurate cross section information

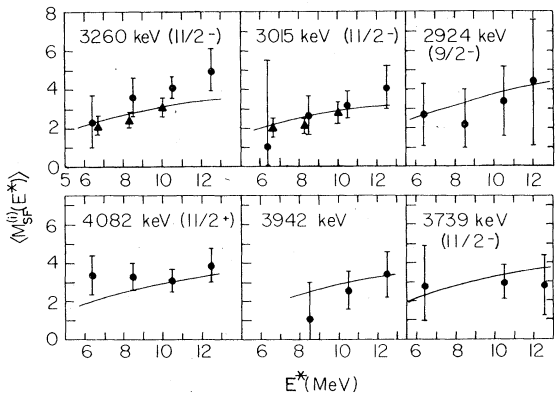

FIG. 1. Comparison of side-feeding multiplicities $\langle M^{(i)}_{\text{SF}}(E^*)\rangle$ measured in this work to compound nucleus calculations. The closed circles refer to the 19.5-MeV experiment, the triangles to the 17.5-MeV experiment. The solid curves are theoretical predictions. Note the agreement in both the trend as a function of excitation energy E^* and the magnitude.

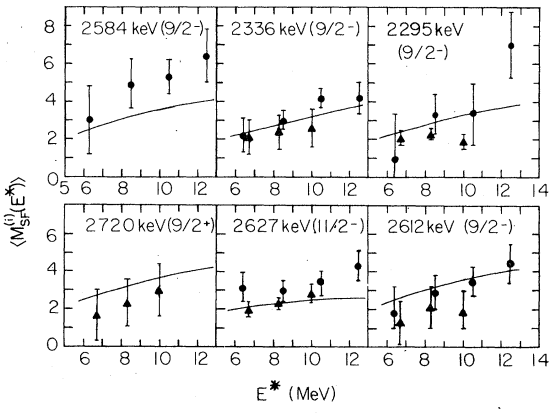

FIG. 2. Comparison of side-feeding multiplicities $\langle M^{(i)}_{\text{SF}}(E^*)\rangle$ measured in this work to compound nucleus calculations. The closed circles refer to the 19.5-MeV experiment, the triangles to the 17.5-MeV experiment. The solid curves are theoretical predictions. Note the agreement in both the trend as a function of excitation energy E^* and the magnitude.

as

$$\langle M^{(i)}_{\text{SF}}(E^*)\rangle = \frac{1}{F^{(i)}_{\text{sf}}}\left(\langle M^{(i)}_{\text{in}}(E^*)\rangle - \sum_{m=i+1}^{l} f_{mi}\left[\langle M^{(m)}_{\text{in}}(E^*)\rangle + 1\right]\right), \quad (8)$$

where $F^{(i)}_{\text{SF}}$ is the side-feeding fraction to the ith state and f_{mi} is the fraction that comes, by way of the mth higher lying state. Clearly $F^{(i)}_{\text{SF}} + \sum_{m=i+1}^{l} f_{mi} = 1$. When $F^{(i)}_{\text{SF}} < 1.0$ and no value is given in parentheses in Tables III and IV then the errors in $\langle M^{(i)}_{\text{in}}(E^*)\rangle$ and/or the cross sections were too large to give a meaningful value for $\langle M^{(i)}_{\text{SF}}(E^*)\rangle$. For the cases where several γ rays deexcite the same level, only their average $\langle M^{(i)}_{\text{in}}(E^*)\rangle$ and $F^{(i)}_{\text{SF}}$ values are used to calculate $\langle M^{(i)}_{\text{SF}}(E^*)\rangle$.

The last column in Tables III and IV gives $\langle M^{(i)}_{\text{in}}\rangle$, the multiplicity of the incoming cascade averaged over E^*, the excitation energy in ^{61}Cu, reached in the 19.5- and 17.0-MeV bombardments.

Total multiplicities $\langle M^{(i)}_{\text{tot}}(E^*)\rangle$ can be obtained from the experimental $\langle M^{(i)}_{\text{in}}(E^*)\rangle$ values of Tables III and IV as $\langle M^{(i)}_{\text{in}}(E^*)\rangle + M_{\text{out}}$.

The results given in Tables III and IV are illustrated in Figs. 1 and 2. The circles and triangles give the values of $\langle M^{(i)}_{\text{SF}}(E^*)\rangle$ from the 19.5- and 17.0-MeV experiments, respectively. It appears that for the region of overlapping excitation energy the values of $\langle M^{(i)}_{\text{SF}}(E^*)\rangle$ to the same level from the two experiments are in agreement within experimental error. The values from the 19.5-MeV experiment, however, reach higher excitation energies and indicate a continuing increase of the

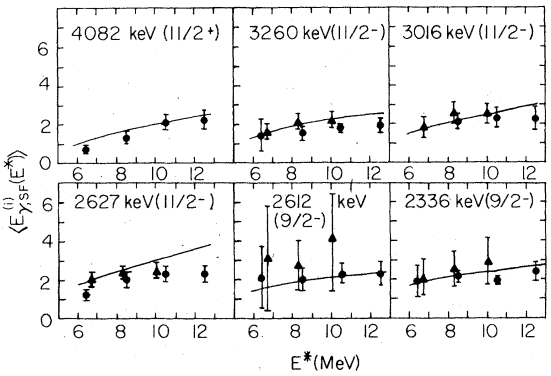

FIG. 3. Average γ-ray energies $\langle E^{(I)}_{\gamma,SF}(E^*)\rangle$ the side-feeding cascades. The circles refer to the 19.5-MeV experiment, and triangles refer to the 19.5- and 17.0-MeV experiments, respectively. The solid curves are the theoretical predictions.

multiplicity $\langle M^{(i)}_{SF}(E^*)\rangle$ with increasing energy E^* of the entry states.

The average γ-ray energy $\langle E^{(i)}_{\gamma,SF}(E^*)\rangle$ for the side-feeding cascade to each level was also obtained in these experiments utilizing Eq. (7). The results are shown in Fig. 3 for some of the levels.

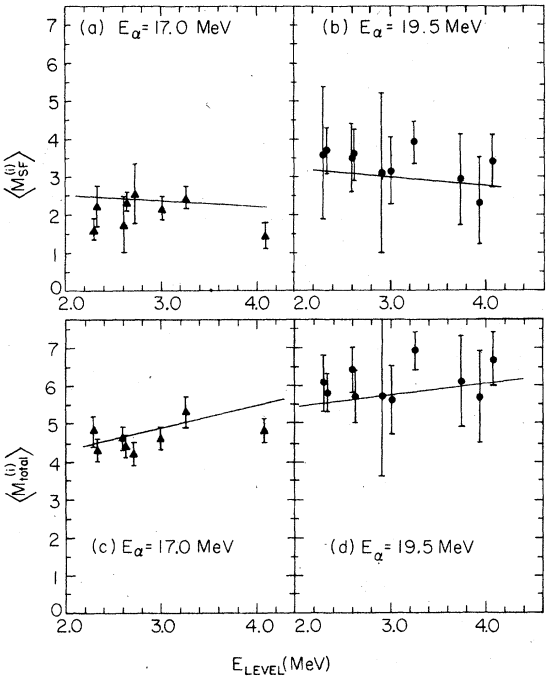

FIG. 4. Side feeding $\langle M^{(i)}_{SF}\rangle$ and total multiplicity $\langle M^{(i)}_{tot}\rangle$ as a function of level energy (a) and (c) from the 17.0-MeV experiment and (b) and (d) from the 19.5-MeV experiment, respectively. The solid curves are the predictions of the theory.

It is seen that the average energy increases from 1.0 to 3.0 MeV when the energy of the entry states increases from 6.0 to 12.5 MeV.

The side feeding multiplicities $\langle M^{(i)}_{SF}\rangle$ averaged over excitation energy for each level i are plotted in Figs. 4(a) and 4(b) as a function of the level energy for the 17.0- and 19.5-MeV bombardments. The 19.5-MeV results suggest a decrease in $\langle M^{(i)}_{SF}\rangle$ with increasing level energy. The total multiplicity $\langle M^{(i)}_{tot}\rangle = \langle M^{(i)}_{in}\rangle + M_{out}$ is plotted in Figs. 4(c) and 4(d) vs. the level energy. It is seen that $\langle M^{(i)}_{tot}\rangle$ rises slightly with increasing energy of the level i.

IV. COMPARISON WITH THEORY

The compound statistical model has been used successfully to explain detailed γ-ray yield information following α bombardments on ^{58}Ni.[3,4] The details of the computer code COMPETITION were presented in Ref. 3. The code generally follows the procedures of Grover and Gilat;[12] however, the code was constructed in such a way that it allows the history of decay to a particular level to be preserved. The code has now been modified to calculate explicitly the side-feeding multiplicity of the γ cascade to each individual discrete level as a function of excitation energy of the entry states.

The calculations performed to analyze the present data are the same with those indicated in Ref. 4. Two different level densities were employed. In the first case level densities derived by a combinatorial technique employing single particle levels obtained from the Wood-Saxon potential were utilized. The calculation of these level densities is discussed in Ref. 13. In the second case, Fermi-gas model level densities were obtained via the expression

$$\rho(U,J) = \frac{1}{12}\left(\frac{\hbar^2}{2I}\right)^{3/2} \frac{a^{1/2}(2J+1)}{(U+t-E_r)^2} \times \exp\{2[a(U-E_r)]^{1/2}\}, \quad (9)$$

where the level spacing parameter a and the thermodynamic temperature t are related by the equation of state $U-\Delta = at^2 - t$. The moment of inertia was parametrized as

$$I(U) = I_{rig}\,[1 - 0.7\exp(-0.693U/d)]\,. \quad (10)$$

The emission rate for γ rays was taken as a sum of contributions from multipoles of order L according to

$$R(EJ, E'J')d\epsilon_\gamma = \sum_L \frac{B(\sigma L)\,\rho(E'J')}{C(\sigma L)\,\rho(EJ)}\,\epsilon_\gamma^{2L+1}\,d\epsilon_\gamma\,, \quad (11)$$

where $B(\sigma L)$ are reduced transition probabilities, $\rho(E'J')$ and $\rho(EJ)$ are the final and initial level

densities, and $C(\sigma L)$ are constants given by[14]

$$C(\sigma L) = \frac{L[(2L+1)!!]^2}{8\pi(L+1)} \frac{\hbar^{2(L+1)} c^{2L+1}}{e^2} . \quad (12)$$

The reduced transition probabilities are parametrized as [W.u. (Weisskopf units)]

$$B(E1) = B_{\text{s.p.}}(E1)[0.001 + b_{E1}(E-4)] \times \frac{E_d^2 + \frac{1}{4}\Gamma^2}{(\epsilon_\gamma - E_d)^2 + \frac{1}{4}\Gamma^2} \text{ (W.u.)}, \quad (13)$$

$$B(M1) = B_{\text{s.p.}}(M1)[0.033 + b_{M1}(E-4)] \text{ (W.u.)}, \quad (14)$$

$$B(E2) = B_{\text{s.p.}}(E2)[10 - b_{E2}(E-4)] \text{ (W.u.)}, \quad (15)$$

$$B(E3) = B_{\text{s.p.}}(E3) \text{ (W.u.)}, \quad (16)$$

with $B_{\text{s.p.}}(E1)/C(E1) = 1.588\times10^{15}$ MeV^{-3} sec^{-1}, $B_{\text{s.p.}}(M1)/C(M1) = 3.149\times10^{13}$ MeV^{-3} sec^{-1}, $B_{\text{s.p.}}(E2)/C(E2) = 1.748\times10^{10}$ MeV^{-5} sec^{-1}, and $B_{\text{s.p.}}(E3)/C(E3) = 1.263\times10^{5}$ MeV^{-7} sec^{-1}. The last factor of Eq. (13) accounts for the giant-dipole-resonance effect.[3] This parametrization allows the reduced transition probabilities to vary from their experimentally determined[2] bound state values to single particle estimates at high excitation.

Figure 5 shows the results of eight calculations for the 3015.6-keV level using different sets of parameters. In Fig. 5(a), the solid curve was calculated with the parameters that gave the best fit to the yield data of Ref. 4. Combinatorial level densities were employed in this calculation and the slopes of the reduced transition rates were $b_{E1} = 0.0041$, $b_{E2} = 0.037$, $b_{M1} = 0.0039$. The dashed line corresponds to increasing b_{E1} to 0.04. The lines corresponding to $b_{E2} = 0.27$, and $b_{M1} = 0.039$ are not drawn, but they lie between the two other lines. It should be noted that changes of this magnitude in the parameters had effects on the cross-section ratios up to 100% but only small effect on the calculated multiplicity. The dash-dot-dash curve corresponds to a calculation using parameters that gave the best fit for the 17.0-MeV experiment. The difference is again seen to be quite small. Figure 5(b) shows a comparison between various choices of the parameter d of Eq. (10). Note that the choice of $d = 3$ MeV yields a moment of inertia approaching rapidly the rigid rotor value. Again it is seen that the calculated multiplicities are quite insensitive to the choice of d. This observation runs counter to the proposal of Ref. 9 that the multiplicity is a sensitive function of the spin cut-off parameter. In Figs. 1 and 2 the solid lines show the calculated multiplicities for those levels for which $\langle M_{\text{SF}}^{(i)}(E^*)\rangle$ could be measured. The theory reproduces not only the observed trend but also the magnitude of the measured multiplicities. In the calculations shown in Figs. 1 and 2 the combinatorial level densities along with the parameters that gave the best fit in Ref. 4 were employed. Theoretical values for the average energy $\langle E_{\gamma,\text{SF}}^{(i)}(E^*)\rangle$ of the γ rays in the side-feeding cascade were obtained as $(E^* - E_{\text{level}})/\langle M_{\text{SF}}^{(i)}(E^*)\rangle$. These are compared with the experimental values in Fig. 3. It is seen that the trend is well reproduced.

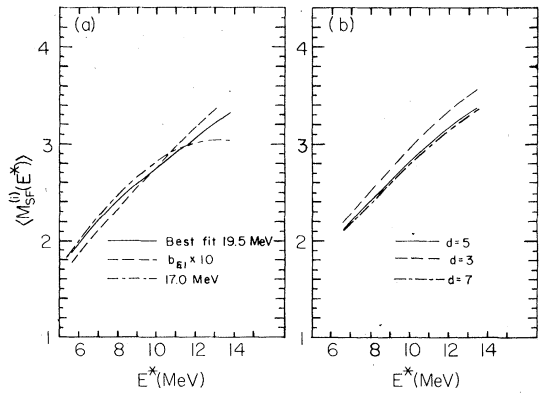

FIG. 5. Theoretical side-feeding multiplicity as a function of E^* for a typical level ($E_{\text{level}} = 2295.0$ keV) for bombardment energy of 19.5 MeV. (a) Combinatorial level densities were employed. The solid curve utilizes the best fit values for the parameters b_{E1}, b_{M1}, b_{E2} [see Eqs. (13)–(15)]. The dashed curve has b_{E1} arbitrarily multiplied by 10. The dash-dot-dash curve repeats the best fit parameter calculation but for a projectile energy of 17 MeV. (b) Best fit parameters for b_{E1}, b_{M1}, b_{E2} were utilized along with Fermi gas level densities. The solid line refers to $d = 5$, the dashed curve to $d = 3$, and the dash-dot-dash curve to $d = 7$ (see Eq. 10).

The calculated multiplicities for individual levels averaged over the excitation energy of the entry states are compared with experiment in Fig. 4. The overall trends in the experimental values for $\langle M_{\text{SF}}^{(i)}\rangle$ and $\langle M_{\text{tot}}^{(i)}\rangle$ as a function of the energy of the level i are well reproduced for both bombardment energies. It is seen that the average multiplicities from the 19.5-MeV experiment are higher by 0.5–1.0 from those of the 17.0-MeV experiment.

The measured multiplicities $\langle M_{\text{SF}}^{(i)}(E^*)\rangle$ refer to levels with J^π values ranging from $\frac{1}{2}^-$ to $\frac{11}{2}^-$. The experimental values of $\langle M_{\text{SF}}^{(i)}(E^*)\rangle$, however, do not exhibit a noticeable correlation with the J^π values of the populated level.

The data of Table III have been averaged over all levels for a given E^* using the observed yields as weights to give $\langle M_{\text{tot}}(E^*)\rangle$. These are presented as open circles in Fig. 6. In the same figure the results of Ref. 9 are represented by another dashed

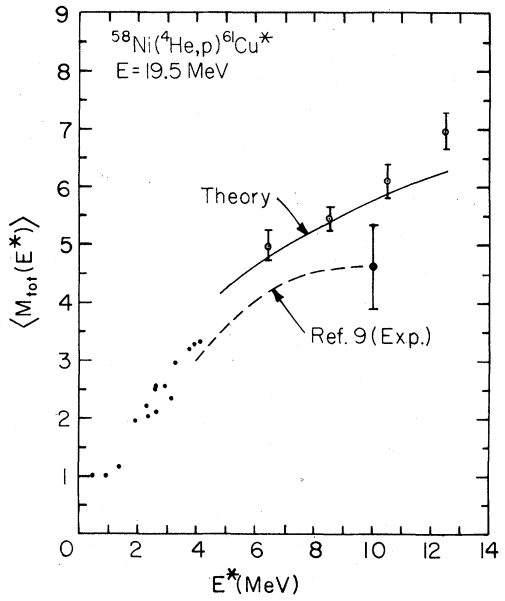

FIG. 6. Average total multiplicity $\langle M_{tot}(E^*)\rangle$ for all cascades starting at excitation energy E^* and ending in the ground state. The open circles refer to the 19.5-MeV experiment. The dashed curve is from the values of Ref. 9. The solid line is from theory. The closed circles are the values for some of the known discrete states below 4100 keV excited in these experiments. A smooth continuation is apparent.

curve drawn through the data points. The error bar on the dashed curve represents the scatter in the data from Ref. 9. Within the large scatter,[9] reasonable agreement is observed although the results from the present work show systematically larger multiplicities at all exciations. In the work of Degnan *et al.*[9] comparable bombardment energies were employed but the present work permitted multiplicity values to be unambiguously extracted for higher excitation energies due to the selectivity of the Ge(Li) detector.

The solid line in Fig. 6 gives the theoretical curve for $\langle M_{tot}(E^*)\rangle$ which is in good agreement with the present results and shows a continuing increase with rising excitation energy. The multiplicities from the continuum at low excitation should merge smoothly with the values from the decay of known discrete states. The latter are shown as closed circles in Fig. 6 substantiating the expected smooth continuation.

V. CONCLUDING REMARKS

The results of the present experiments, as illustrated in Figs. 1–4 show that the compound statistical model is capable of detailed predictions of the multiplicity of the γ rays involved in the deexcitation of nuclei formed at energies below ≃ 20.0 MeV. The good agreement between the model predictions and experiment lend further strength to the belief that the compound statistical model is describing the reaction correctly. Within the context of this model one can draw conclusions about the details of the (^{4}He, p) reactions and subsequent γ decay. A comparison of the data for the two bombarding energies in Figs. 1 and 2 leads to the conclusion that the shape of the spin distributions for the same residual excitation energy are not greatly different for these two bombarding energies. This is based on the observation that the multiplicities from the two bombarding energies show essentially the same dependence on excitation energy of the entry states. Obviously the magnitude of the populations need not be the same. As expected the 19.5-MeV bombardment reaches higher excitations at which the spin distributions extend to higher J values as evidenced by the continued increase of $\langle M_{SF}^{(i)}(E^*)\rangle$ with increasing excitation. The lack of sensitivity of the calculated values of $\langle M_{SF}^{(i)}(E^*)\rangle$ to the choice of parameters controlling the theoretical γ strength can be understood in terms of the fact that the number of so-called statistical γ rays depends only on ratios of level densities at different excitations and it is thus unaffected by the absolute transition rate for a given multipole. For excitation energies reached in this work, the yrast cascade is rather short and includes only a few of the γ rays in the cascade. The small number of yrast transitions also accounts for the insensitivity of $\langle M_{SF}^{(i)}(E^*)\rangle$ to the exact location of the yrast line, i.e., the insensitivity of $\langle M_{SF}^{(i)}(E^*)\rangle$ to the moment of inertia.

ACKNOWLEDGMENTS

We would like to thank Dr. David C. Hensley for his help with programming in the initial data reduction stage. The excellent cooperation of the operating staff of the Washington University cyclotron and Uppsala tandem accelerator is greatly appreciated.

*Work supported in part by the U. S. Energy Research and Development Administration.
†Work supported in part by the Research Corporation.

[1]E. J. Hoffman and D. G. Sarantites, Phys. Rev. 177, 1647 (1967).
[2]D. G. Sarantites, J. H. Barker, N.-H. Lu, E. J. Hoffman, and D. M. Van Patter, Phys. Rev. C 8, 629 (1973).

[3]E. J. Hoffman and D. G. Sarantites, Nucl. Phys. A180, 177 (1972).
[4]J. H. Barker and D. G. Sarantites, Phys. Rev. C 9, 607 (1974).
[5]D. G. Saranties, J. H. Barker, and N.-H. Lu, Phys. Rev. C 9, 603 (1974).
[6]P. O. Tjøm, F. S. Stephens, R.M. Diamond, J. de Boer, and W. E. Meyerhof, Phys. Rev. Lett. 33, 593 (1974).
[7]G. B. Hagemann, R. Broad, B. Herskind, M. Ishihara, S. Ogaza, and H. Ryde, Nucl. Phys. A245, 166 (1975).
[8]D. G. Sarantites, J. H. Barker, M. L. Halbert, D. C. Hensley, R. A. Dayras, E. Eichler, N. R. Johnson, and S. A. Gronemeyer, Phys. Rev. C 14, 2138 (1976).
[9]J. H. Degnan, B. L. Cohen, G. R. Rao, K. C. Chan, and L. Shabason, Phys. Rev. C 8, 2255 (1973).
[10]L. Westerberg, D. G. Sarantites, R. Lovett, J. T. Hood, J. H. Barker, C. M. Currie, and N. Mullami, Nucl. Instrum. Methods 145, 295 (1977).
[11]K. S. Krane, R. M. Steffen, and R. M. Wheeler, Nucl. Data A11, 407 (1973).
[12]J. R. Grover and J. Gilat, Phys. Rev. 157, 803 (1967).
[13]G. P. Ford, D. C. Hoffman, and E. Rost, Los Alamos Scientific Laboratory Report No. LA-4329 (unpublished).
[14]A factor of $1/8\pi(L+1)$ was omitted in Eq. (4) in Ref. 4.